

Carboxylic Acid Deprotonation on the Ag(110) and Ag(111) Surfaces

Bryan Parker

Department of Chemistry, University of Illinois, Urbana, Illinois 61801

Boonchuan Immaraporn[†] and Andrew J. Gellman^{*‡}

Departments of Chemistry and of Chemical Engineering, Carnegie Mellon University, Pittsburgh, Pennsylvania 15213

Received July 16, 2001

The surface chemistry of hydrocarbon carboxylic acids has been compared with that of perfluorinated carboxylic acids on the Ag(110) and Ag(111) surfaces. The hydrocarbon acids adsorb reversibly on the clean silver surfaces. On Ag(110) their desorption energies increase linearly with increasing alkyl chain length (n) and are given by the expression $\Delta E_{\text{des}} = 10.6 + 0.9n$ kcal/mol. The surface chemistry of the perfluorinated acids is quite different from that of the hydrocarbon acids in the sense that they deprotonate to form perfluorocarboxylate species on both Ag(110) and Ag(111) surfaces. The perfluorocarboxylates are stable until the surface temperature reaches ~ 620 K, at which point they decompose yielding desorption of CO_2 and other decomposition fragments. On both Ag surfaces 2,2,2-trifluoroacetate (CF_3CO_2) generated by deprotonation of 2,2,2-trifluoroacetic acid ($\text{CF}_3\text{CO}_2\text{H}$) has been identified by its vibrational spectrum. The fact that fluorinated acids deprotonate on the Ag surfaces while the hydrocarbon acids desorb during heating indicates that fluorination lowers the deprotonation barrier, $\Delta E_{\text{dep}}^\ddagger$, to the point that it is lower than the desorption energy, ΔE_{des} .

1. Introduction

The kinetics of complex chemical reactions are determined by the transition states to elementary chemical reaction steps and the associated reaction barriers, ΔE^\ddagger . As a result, understanding the nature of the transition state is central to the understanding of chemical reaction kinetics in the gas phase, in solution phase, and on solid surfaces. For catalytic reactions occurring on solid surfaces such understanding will guide manipulation of reaction conditions or reaction pathways in order to increase catalytic activities and improve selectivities. Unfortunately, it is extremely difficult to attempt to detect the transition state for a reaction on a solid surface directly. This paper describes an effort to probe the nature of the transition state to the deprotonation of acids on surfaces through an indirect approach, the use of substituent effects.

The nature of the transition states of several surface reactions has been studied by employing field substituent effects.¹ As an example, β -hydride elimination in hydrocarbon alkoxides on the Cu(111) surface ($\text{RCH}_2\text{O}-\text{Cu} \rightarrow \text{RCH}=\text{O} + \text{H}-\text{Cu}$) has been shown to have a transition state in which the β -carbon atom is cationic, $[\text{C}^{\delta+}\cdots\text{H}]^\ddagger$, with respect to the initial state alkoxide.^{2–4} In that work, fluorinating the substituent (R) of the alkoxides increases its local dipole moment or field effect and destabilizes the positive charge on the β -carbon in the transition state. As a result, fluorination increases the activation barrier to β -hydride elimination, $\Delta E_{\beta\text{-H}}^\ddagger$. If the transition state had

been anionic, $[\text{C}^{\delta-}\cdots\text{H}]^\ddagger$, then $\Delta E_{\beta\text{-H}}^\ddagger$ would have been decreased by fluorination of the substituent. As another example of the use of substituent effects, the transition state for C–I bond breaking in alkyl iodides ($\text{R}_3\text{C}-\text{I}$) on Ag(111) and Pd(111) surfaces has been studied via fluorination of the substituent alkyl groups (R).^{5–7} On the Ag(111) surface the transition state for C–I bond breaking has been shown to be slightly anionic with respect to the initial state ($\text{R}_3\text{C}-\text{I} \rightarrow [\text{R}_3\text{C}^{\delta-}\cdots\text{I}]^\ddagger$). In this reaction fluorination of the alkyl substituent groups lowers the activation barrier for C–I cleavage, $\Delta E_{\text{C-I}}^\ddagger$, by stabilizing the anionic transition state with respect to the initial state. The effect is quite small but clearly significant. On the basis of these and other studies, it appears that fluorine substituent effects are generally useful for probing the nature of the transition states to surface reactions.¹

The work presented in this paper probes the nature of the transition state for carboxylic acid deprotonation on the Ag(111) and Ag(110) surfaces by comparing the kinetics of deprotonation in hydrocarbon and fluorocarbon acids. Acid deprotonation is a fairly simple reaction which has been studied on a number of metal surfaces and is a reaction which one can imagine occurs by a single elementary step. Previous work has documented the surface chemistry of hydrocarbon acids; however, little has been done to study the fluorinated acids on metal surfaces. By contrast, the kinetics and equilibria for deprotonation in the gas phase or solution phase have been studied extensively in a wide range of hydrocarbon and partially fluorinated acids.⁸ As a result, fluorine substituent effects on the gas phase heats of deprotonation

[†] Department of Chemistry

[‡] Department of Chemical Engineering.

* To whom correspondence should be sent.

(1) Gellman, A. J. *Acc. Chem. Res.* **2000**, *33*, 19.

(2) Gellman, A. J.; Dai, Q. *J. Am. Chem. Soc.* **1993**, *115*, 714.

(3) Dai, Q.; Gellman, A. J. *J. Phys. Chem.* **1993**, *97*, 10783.

(4) Gellman, A. J.; Buelow, M. T.; Street, S. C.; Morton, T. H. *J. Phys. Chem. A* **2000**, *104*, 2476.

(5) Buelow, M. T.; Immaraporn, B.; Zhou, G.; Gellman, A. J. *Catal. Lett.* **1999**, *59*, 9.

(6) Buelow, M. T.; Gellman, A. J. *J. Am. Chem. Soc.* **2001**, *123*, 1440.

(7) Buelow, M. T.; Immaraporn, B.; Gellman, A. J. *J. Catal.*, in press.

(8) Bartmess, J. E.; McIver, R. T., Jr. In *Gas-Phase Ion Chemistry*; Bowers, M. T., Ed.; Academic Press: New York, 1977; Vol. 2, Chapter 11, p 87.

have been measured and are available for comparison with the energetics of deprotonation on surfaces. As an example, the heat of deprotonation of 2,2,2-trifluoroacetic acid ($\text{CF}_3\text{CO}_2\text{H}$) in the gas phase is 25 kcal/mol lower than the heat of acetic acid ($\text{CH}_3\text{CO}_2\text{H}$) deprotonation.⁸ This suggests that if the process is also ionic on surfaces, $\Delta E_{\text{dep}}^\ddagger$ might be lower in $\text{CF}_3\text{CO}_2\text{H}$ than in $\text{CH}_3\text{CO}_2\text{H}$. The existing body of knowledge concerning acid chemistry in the gas phase and on surfaces makes deprotonation an ideal reaction for use of substituent effects as a probe of the transition state.

The chemistry of carboxylic acids on single-crystal transition metal surfaces has been widely studied.^{9–17} Deprotonation of these acids to form carboxylates has been observed on clean metal surfaces.^{11–17} The carboxylate later decomposes to yield CO_2 and other hydrocarbon products. The motivation behind previous work has been that the formation of a carboxylate intermediate is important in several catalytic reactions, e.g., alcohol synthesis and the methanation of CO ^{18,19} and CO_2 .^{20–22} Because the chemistry of $\text{CH}_3\text{CO}_2\text{H}$ on Ag surfaces has been studied previously,^{9–11} these surfaces are good candidates for the study carried out in this work. On the clean Ag(110) surface $\text{CH}_3\text{CO}_2\text{H}$ adsorbs reversibly at low temperatures and desorbs into the gas phase during heating without ever deprotonating.⁹ In order for deprotonation to occur, the Ag(110) surface must be oxidized prior to $\text{CH}_3\text{CO}_2\text{H}$ adsorption. Deprotonation of $\text{CH}_3\text{CO}_2\text{H}$ on the preoxidized Ag(110) surface results in the formation of a stable acetate (CH_3CO_2^-) intermediate. During heating the CH_3CO_2^- decomposes at $T \sim 600$ K to yield CO_2 , CH_4 , $\text{CH}_3\text{CO}_2\text{H}$, and ketene which desorb into the gas phase.¹⁰ Similarly on the Ag(111) surface, $\text{CH}_3\text{CO}_2\text{H}$ only deprotonates on the preoxidized surface.¹¹ The nature of the transition state for the deprotonation reaction has not been addressed in previous work. This paper will describe the first attempt to probe the nature of the transition state for deprotonation of acids on Ag(110) and Ag(111) surfaces.

An experimental study of the effects of fluorination and alkyl chain length on the deprotonation of carboxylic acids on Ag(110) and Ag(111) surfaces is described in this article. These results show that while hydrocarbon acids desorb from the clean surfaces, the fluorinated acids deprotonate to form fluorinated carboxylates. The same chemistry is observed for these acids on both Ag surfaces. These results indicate that $\Delta E_{\text{dep}}^\ddagger$ of the fluorinated acids is lower than that of the hydrocarbon acids.

2. Experimental Section

The experiments performed on the Ag(110) surface were done in two ultrahigh-vacuum (UHV) chambers. Both are equipped with ion guns for cleaning the crystal surface, electron optics for

low-energy electron diffraction (LEED), and Auger electron spectroscopy (AES), leak valves for gas dosing, and Dycor quadrupole mass spectrometers for desorption measurements. The chamber used for the study on the Ag(110) surface is also equipped with a high-resolution electron energy loss (HREEL) spectrometer. The experiments performed on the Ag(111) surface were conducted in a different chamber equipped with a Mg $K\alpha$ X-ray source and a VG CLAM II hemispherical analyzer for X-ray photoelectron spectroscopy (XPS). In addition, that chamber was equipped with a Mattson RS-1 FTIR spectrometer with a narrow-banded HgCdTe detector used for Fourier transform infrared reflection-absorption spectroscopy.

The Ag single-crystal samples were purchased from Monocrystals Inc. and were mounted by spot-welding between two Ta wires on small sample holders which were then bolted to the ends of the UHV manipulators. The manipulators allow cooling of the samples to $T < 100$ K and resistive heating to $T > 1000$ K. Chromel–alumel thermocouples were spot-welded to the edges of the Ag samples for temperature measurement. The silver samples were cleaned by several cycles of Ar^+ sputtering followed by annealing to 800 K. Deposits of carbon on the Ag(110) surface resulting from the decomposition of acetates were removed by exposing the crystal to 5 langmuirs of O_2 while it was heated to 300 K. Adsorbed oxygen atoms react with carbon to produce CO_2 , which desorbs with a peak maximum at about 480 K. Unreacted oxygen atoms recombine to desorb as O_2 at 550 K. The Ag(110) surface was judged to be free of carbon when no CO_2 was detected by temperature-programmed desorption following oxygen adsorption. Because the Ag(111) surface does not readily adsorb oxygen, it could only be cleaned by using Ar^+ sputtering. XPS was used to monitor the cleanliness of the Ag(111) surface.

The experiments used a series of straight-chain hydrocarbon and fluorocarbon carboxylic acids obtained from Aldrich Chemical Co., Inc. The acids are all liquids and were purified by several cycles of freeze–pump–thawing. The purity of the vapor introduced into the UHV chamber through the leak valves was verified by mass spectrometry. The acids were adsorbed on the clean surfaces at 90 K by backfilling the chamber through a leak valve.

Temperature-programmed desorption (TPD) and temperature-programmed reaction spectroscopy (TPRS) were performed using the Dycor mass spectrometers. After preparation of the adsorbate layers on the Ag surfaces they were positioned in front of the mass spectrometer and heated. The heating rates were 5 and 2 K/s for Ag(110) and Ag(111) samples, respectively. A computer was used to control the heating and to record the temperature during TPD experiments. The mass spectrometer was capable of monitoring the signals for as many as five different m/q ratios simultaneously.

X-ray photoelectron spectroscopy was performed on the Ag(111) surface. The X-ray source power was 600 W, and the analyzer was used with a pass energy of 100 eV throughout all the XPS experiments. The scan times were approximately 15 min for the C 1s and O 1s spectra, 5 min for the F 1s spectra, and 1 min for the Ag 3d spectra. Spectral acquisition times substantially greater than this induced noticeable X-ray damage of the $\text{CF}_3\text{CO}_2\text{H}$. The binding energies of the XPS peaks were scaled assuming that the values for the Ag peaks were Ag 4s = 98 eV, Ag 3d_{5/2} = 368 eV, Ag 3d_{3/2} = 374 eV, Ag 3p_{3/2} = 573 eV, and Ag 3p_{1/2} = 604 eV.²³

The FT-IRRAS spectra were obtained from the Ag(111) surface using a single reflection of the infrared beam at grazing incidence. The Mattson RS-1 spectrometer was operated at a resolution of 4 cm^{-1} . A polarization elastic modulator (PEM) was used with the modulated wavelength at 1800 cm^{-1} . Both the difference and the sum interferograms were collected using 2000 scans for each. The differential reflectance spectrum was obtained by taking the ratio of the difference and the sum interferograms when the surface was clean and in the presence of adsorbed species. The absorbance spectra are then the ratios of these differential reflectance spectra.

The HREEL spectra were obtained from the Ag(110) surface using an LK-2000 spectrometer. All spectra were obtained with

- (9) Barteau, M. A.; Bowker, M.; Madix, R. J. *Surf. Sci.* **1980**, *94*, 303.
 (10) Barteau, M. A.; Bowker, M.; Madix, R. J. *J. Catal.* **1981**, *67*, 118.
 (11) Sim, W. S.; Glardner, P.; King, D. A. *J. Am. Chem. Soc.* **1996**, *118*, 9953.
 (12) Bowker, M.; Madix, R. J. *Appl. Surf. Sci.* **1981**, *8*, 299.
 (13) Davis, J. L.; Barteau, M. A. *Surf. Sci.* **1991**, *256*, 50.
 (14) Madix, R. J.; Falconer, J. L.; Suszko, A. M. *Surf. Sci.* **1976**, *54*, 6.
 (15) Schoofs, G. R.; Benziger, J. B. *Surf. Sci.* **1984**, *143*, 359.
 (16) Erely, W.; Chen, J. G.; Samder, D. *J. Vac. Sci. Technol. A* **1990**, *8*, 976.
 (17) Avery, N. R. *J. Vac. Sci. Technol.* **1982**, *20*, 592.
 (18) Solymosi, F.; Tombacz, I.; Kocsis, M. *J. Catal.* **1982**, *75*, 78.
 (19) Ichikawa, M.; Shikakura, K. *Proc. 7th Int. Congr. Catal.* Tokyo, Part B, p 925.
 (20) Solymosi, F.; Erdohelyi, A.; Kocsis, M. *J. Catal.* **1980**, *65*, 428.
 (21) Solymosi, F.; Erdohelyi, A.; Bansagi, T. *J. Catal.* **1981**, *68*, 371.
 (22) Hernderson, M. A.; Woorley, S. D. *J. Phys. Chem.* **1985**, *89*, 1417.
 (23) Wagner, C. D.; Riggs, W. M.; Davis, L. E.; Moulder, J. F.; Muilenberg, G. E., Eds.; *Handbook of X-ray Photoelectron Spectroscopy*; Perkin-Elmer Corporation: Eden, Prairie, MN, 1979.

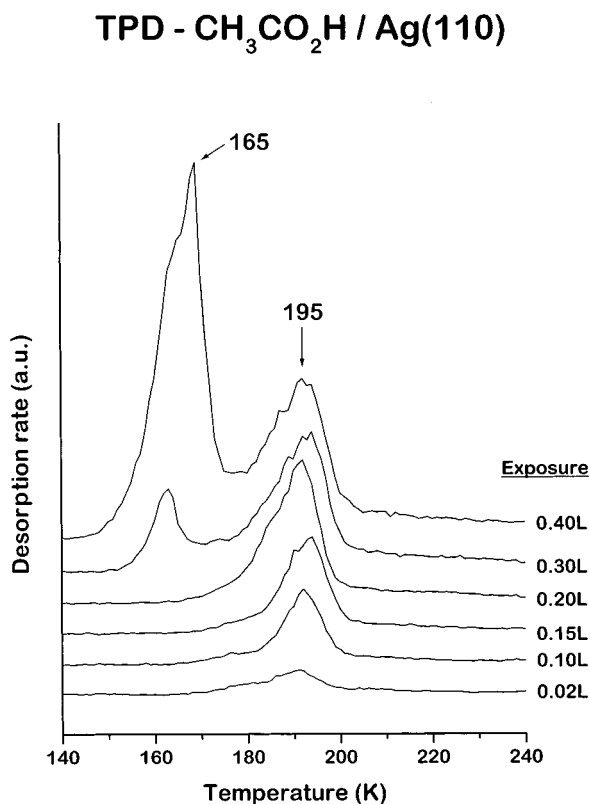


Figure 1. TPD spectra of CH₃CO₂H on the Ag(110) surface at increasing coverages. At low coverages a single desorption feature is observed at 192 K due to desorption of the adsorbed monolayer. At the higher coverages the multilayer desorption feature is observed at 162 K. The exposures were made at a surface temperature of 120 K using a capillary array doser. The heating rate was 5 K/s, and the fragment monitored had $m/q = 44$ amu.

the surface at a temperature of 90 K. The primary beam energy was 1.3 eV, and the spectra were obtained using multiple scans with a total dwell time of 3.0 s/pt.

3. Results

3.1. Carboxylic Acid on the Clean Silver Surfaces.

CH₃CO₂H adsorbs and desorbs reversibly on both the clean Ag(110) and Ag(111) surfaces. Figure 1 shows the TPD spectra of CH₃CO₂H adsorbed on Ag(110) at increasing exposures. The CH₃CO₂H monolayer desorbs at $T = 195$ K with a coverage-independent peak maximum, indicating first-order desorption kinetics.²⁴ Following saturation of the monolayer, further adsorption results in formation of a condensed multilayer which desorbs at 165 K and exhibits zero-order desorption kinetics. CH₃CO₂H adsorption on the clean Ag(111) surface exhibits the same reversible adsorption with the monolayer desorbing at $T = 200$ K. The fact that CH₃CO₂H desorbs from the Ag(111) surface without decomposition is illustrated by the C 1s and O 1s X-ray photoemission spectra of Figures 2 and 3. The C 1s spectrum taken at 90 K for the adsorbed CH₃CO₂H monolayer reveals two peaks: one at a binding energy of 288.5 eV from the carbon of the methyl group and the other at 292.5 eV from the carbon of the carboxyl group. This splitting was also observed in a study on the Cu(110) surface which reported binding energies of 286.6 and 290.0 eV for the carbon atoms in the methyl group and carboxyl groups, respectively.¹² The O 1s photoemission spectrum of the adsorbed CH₃CO₂H monolayer is

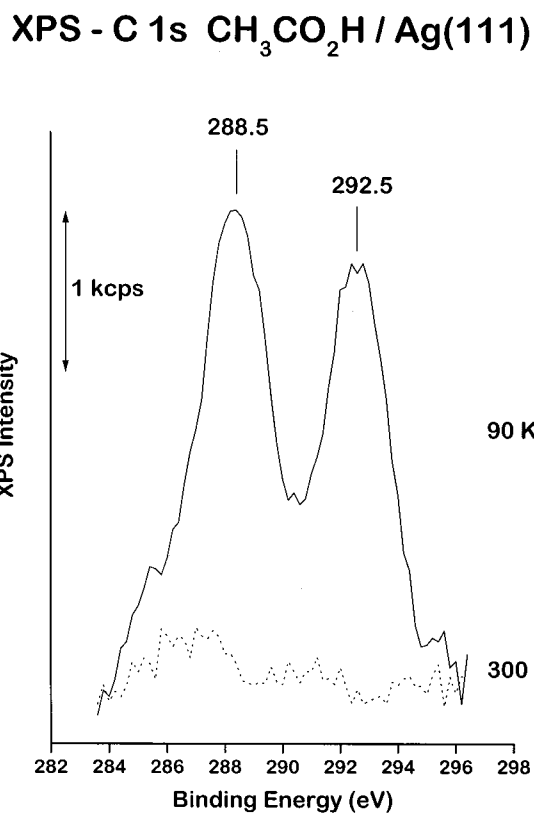


Figure 2. XPS of the C 1s region for an CH₃CO₂H monolayer adsorbed on the Ag(111) surface at 90 K and for the surface after heating to 300 K. The two features in the monolayer spectrum are assigned to the -CH₃ group (binding energy = 288.5 eV) and to the -CO₂H group (binding energy = 292.5 eV). After heating the surface to 300 K all the CH₃CO₂H has desorbed.

shown in Figure 3 and shows a single feature with a binding energy of 535.2 eV. Both Figures 2 and 3 reveal that heating the surface to 300 K results in the desorption of the CH₃CO₂H and leaves the Ag(111) surface clean.

In addition to CH₃CO₂H the longer, straight-chain carboxylic acids have been studied on the Ag(110) surface. These have included acetic through to hexanoic acid, CH₃(CH₂)₄CO₂H. In all cases these are also observed to adsorb and desorb reversibly from the clean Ag(110) surface. Figure 4 shows the desorption of adsorbed monolayers of the straight-chain carboxylic acids from the clean Ag(110) surface. The peak desorption temperature increases by roughly 10–15 K per additional methylene group in the alkyl chain. Using the Redhead equation and estimating that the desorption preexponential factor is 10^{13} s^{-1} allows us to estimate the desorption energies, ΔE_{des} , of the acids.²⁴ These are plotted in Figure 5 and reveal that the desorption energies increase by ~ 0.9 kcal/mol of CH₂ with the form $\Delta E_{\text{des}} = 10.6 + 0.9n$ kcal/mol, where n is the number of carbon atoms in the alkyl chain.

As observed in previous work, it is only possible to deprotonate CH₃CO₂H on the Ag(110) and Ag(111) surfaces by first partially oxidizing the surface.¹¹ The adsorbed oxygen atom acts as a Bronsted base and deprotonates the acid to produce acetate, CH₃CO₂. During heating the CH₃CO₂ decomposes to produce CO₂, CH₄, and other species at temperatures on the order of 600 K. We have also observed that CH₃CO₂H is deprotonated on the oxidized Ag(110) surface and decomposes to produce CO₂ at high temperatures.²⁵

(24) Redhead, P. A. *Vacuum* **1962**, *12*, 203.

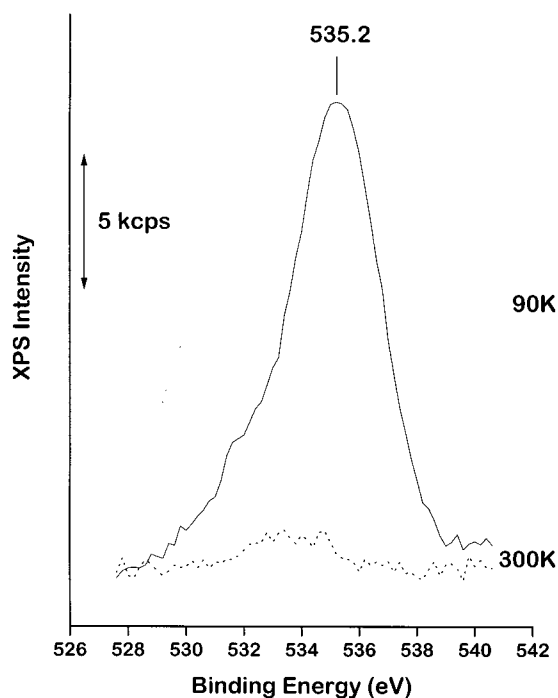
XPS - O 1s $\text{CH}_3\text{CO}_2\text{H} / \text{Ag}(111)$ 

Figure 3. XPS of the O 1s region for an $\text{CH}_3\text{CO}_2\text{H}$ monolayer adsorbed on the Ag(111) surface at 90 K and for the surface after heating to 300 K. The spectrum exhibits one single broad feature at a binding energy of 535.2 eV for both oxygen atoms in the $-\text{CO}_2\text{H}$ group. After heating to 300 K all the $\text{CH}_3\text{CO}_2\text{H}$ has desorbed from the surface.

3.2. Perfluorinated Carboxylic Acids on Clean Ag Surfaces. The surface chemistry of the perfluorinated carboxylic acids on the clean Ag(110) and Ag(111) surfaces appears to be quite different from that of the hydrocarbon carboxylic acids. Whereas the hydrocarbon acids are reversibly adsorbed on the clean surface and desorb during heating, the perfluorinated acids all deprotonate to produce perfluorocarboxylates.

The desorption of $\text{CF}_3\text{CO}_2\text{H}$ from the clean Ag(111) surface is shown in Figure 6 as a function of increasing coverage. These TPRS spectra have been obtained by monitoring the signal at $m/q = 44$ with the mass spectrometer. At low temperatures these TPR spectra reveal a desorption feature at ~ 230 K which is probably due to desorption of the $\text{CF}_3\text{CO}_2\text{H}$ monolayer and at the highest coverage a narrow desorption feature at 145 K that is due to desorption of the $\text{CF}_3\text{CO}_2\text{H}$ multilayer. The most important thing to note is the desorption feature at 640 K that is not present in the desorption spectra of $\text{CH}_3\text{CO}_2\text{H}$. Additional ionization fragments observed in the spectrum of the species desorbing at 630 K include $m/q = 69$, (CF_3^+), 50 (CF_2^+), and 31 (CF^+). This feature occurs at a similar temperature to that observed during the decomposition of CH_3CO_2 generated by $\text{CH}_3\text{CO}_2\text{H}$ adsorption on the oxidized Ag(110) surface and suggests that some of the $\text{CF}_3\text{CO}_2\text{H}$ has deprotonated to form trifluoroacetate, CF_3CO_2 . The important point is that in the case of $\text{CF}_3\text{CO}_2\text{H}$ this has occurred on the *clean* Ag(111) surface. The same reaction appears to occur on the *clean* Ag(110) surface. Figure 7 shows the desorption

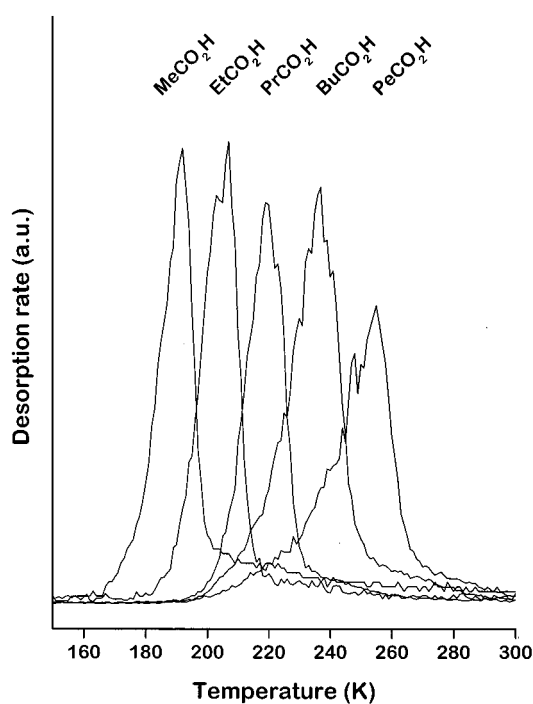
TPD - $\text{RCO}_2\text{H} / \text{Ag}(110)$ 

Figure 4. TPD spectra for monolayers of the straight chain carboxylic acids $\text{H}(\text{CH}_2)_n\text{CO}_2\text{H}$ ($n = 1-5$) adsorbed on the clean Ag(110) surface at 90 K. The peak desorption temperatures increase by 10–15 K per CH_2 group in the alkyl chain. The heating rate was 5 K/s, and the fragment monitored had $m/q = 44$ amu.

spectra for perfluoro-acetic, -propionic, and -butanoic acids on the clean Ag(110) surface. These all reveal the same high-temperature desorption feature observed in the case of $\text{CF}_3\text{CO}_2\text{H}$ on the clean Ag(111) surface and suggest that all three are undergoing deprotonation to form perfluorinated carboxylates on the Ag(110) surface.

One interesting point is that we have never been able to determine the fate of the proton that must be lost during the conversion of the fluorinated acids to the fluorinated carboxylates. It does not appear in the desorption spectra as either H_2 or H_2O . While it is possible that it dissolves into the bulk of the Ag samples this seems unlikely. It is possible that it desorbs during the adsorption process. If that is the case, then it implies that deprotonation is occurring at the adsorption temperature of 90 K.

3.3. CF_3CO_2 on Ag(111) and Ag(110). The deprotonation of the perfluorinated carboxylic acids on the Ag(110) and Ag(111) surfaces ought to result in the production of perfluorinated carboxylates. In particular, the deprotonation of $\text{CF}_3\text{CO}_2\text{H}$ should result in the production of CF_3CO_2 . Evidence for this comes from the XP spectra. Figures 8 and 9 show the C 1s and O 1s XP spectra of a $\text{CF}_3\text{CO}_2\text{H}$ monolayer adsorbed on the Ag(111) surface at 90 K and after heating to 300 K. The spectrum of the monolayer at 90 K reveals poorly resolved features with binding energies of 293.5 eV for the carboxyl group and 295.8 eV for the $-\text{CF}_3$ group. During heating it is quite clear that roughly 75% of the $\text{CF}_3\text{CO}_2\text{H}$ desorbs from the surface; however, there is still carbon and oxygen left after heating to 300 K. The C 1s spectrum still reveals the presence of two features although they are now shifted to 294.4 and 291.1 eV. The O 1s feature shows a single broad peak that shifts from 535.5 to 533.5 eV binding energy

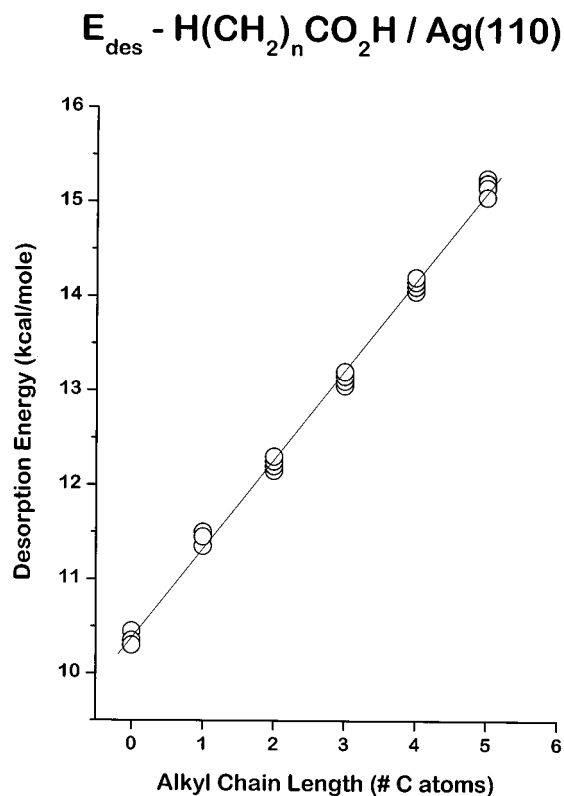


Figure 5. Desorption energies (ΔE_{des}) of the straight-chain carboxylic acids $\text{H}(\text{CH}_2)_n\text{CO}_2\text{H}$ ($n = 1-5$) adsorbed on the clean $\text{Ag}(110)$. The values of ΔE_{des} were estimated by using the Redhead equation with the peak desorption temperatures obtained from the monolayer TPD spectra and the assumption that the desorption preexponential was $\nu = 10^{13} \text{ s}^{-1}$. The ΔE_{des} are fit by the line $\Delta E_{\text{des}} = 10.6 + 0.9n \text{ kcal/mol}$.

and also loses about 75% of its intensity on heating from 90 to 300 K. Although this is not shown, there is also fluorine left on the surface. It is important to note that the XP spectra shown in Figures 2 and 3 for $\text{CH}_3\text{CO}_2\text{H}$ on the $\text{Ag}(111)$ surface reveal that all the $\text{CH}_3\text{CO}_2\text{H}$ had desorbed from the surface after heating to 300 K. Further evidence that heating adsorbed $\text{CF}_3\text{CO}_2\text{H}$ generates adsorbed CF_3CO_2 comes from the fact that the stoichiometry of the surface species remains $\text{F}:\text{C}:\text{O} \approx 3:2:2$ on heating from 90 to 500 K.

$\text{CF}_3\text{CO}_2\text{H}$ and the decomposition intermediate believed to be CF_3CO_2 have been studied using HREELS on the $\text{Ag}(110)$ surface and FT-IRRAS on the $\text{Ag}(111)$ surface. Figure 10 shows the HREEL spectra for a $\text{CF}_3\text{CO}_2\text{H}$ multilayer on the $\text{Ag}(110)$ surface and the species present after annealing to 500 K. Many of the modes observed in the multilayer spectrum can be assigned to vibrational modes observed in gas-phase $\text{CF}_3\text{CO}_2\text{H}$.²⁶ These assignments and the mode frequencies are listed in Table 1. The primary feature in the multilayer HREEL spectrum is an unresolved combination of the $\nu_{\text{CF}_3^s}$, $\nu_{\text{CF}_3^a}$, ν_{CO} , and δ_{OH} modes at 1210 cm^{-1} . Once the surface has been heated to 500 K the spectrum becomes simpler, and the modes can be assigned to those that are observed in an aqueous solution of sodium 2,2,2-trifluoroacetate ($\text{CF}_3\text{CO}_2\text{Na}$).^{27,28} The assignments are listed in Table 2. The modes due to vibrations of the carboxylate group are absent, but the primary feature due to the ν_{CF_3} modes is still present

TPD - $\text{CF}_3\text{CO}_2\text{H} / \text{Ag}(111)$

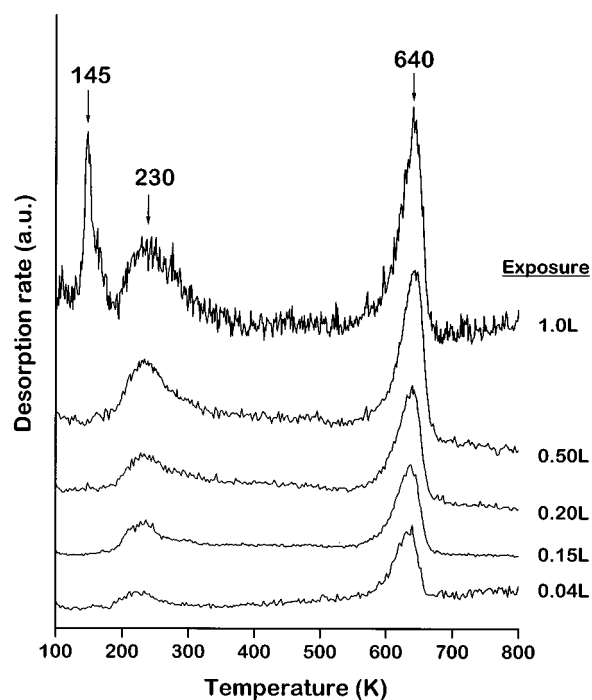


Figure 6. TPD spectra of $\text{CF}_3\text{CO}_2\text{H}$ adsorbed on the $\text{Ag}(111)$ surface at varying coverages. At the lower coverages there is evidence of a monolayer desorption feature at 230 K and then a high-temperature desorption features at 635 K that is due to the decomposition of CF_3CO_2 generated by deprotonation of the $\text{CF}_3\text{CO}_2\text{H}$. This feature is not observed at all in the TPD spectra of $\text{CH}_3\text{CO}_2\text{H}$ on the $\text{Ag}(111)$ surface. At the highest exposure there is a narrow desorption feature at 150 K that is attributed to multilayer desorption. The heating rate was 2 K/s , and the fragment monitored was at $m/q = 44$.

although it is too broad to resolve contributions from the symmetric and asymmetric components. In the low-frequency regions the spectra of $\text{CF}_3\text{CO}_2\text{H}$ and CF_3CO_2 are quite similar, and it would be quite difficult to distinguish between the two on the basis of the frequencies of modes below 1500 cm^{-1} . The primary difference which suggests the formation of CF_3CO_2 from the acid is that the feature due to the ν_{CF_3} modes has red-shifted by about 30 cm^{-1} . In the reference spectra the $\nu_{\text{CF}_3^s}$ and $\nu_{\text{CF}_3^a}$ modes are both red-shifted by about 40 cm^{-1} on going from gas-phase $\text{CF}_3\text{CO}_2\text{H}$ to aqueous $\text{CF}_3\text{CO}_2\text{Na}$.²⁶⁻²⁸ The other feature which reveals that the low-temperature species is the molecular acid is the loss at 3020 cm^{-1} which is due to the O-H stretch. This feature is not observed in the spectrum of the species thought to be CF_3CO_2 produced by heating to 500 K. Finally, it is interesting to note that the loss features at $1300-1500 \text{ cm}^{-1}$ in the HREEL spectrum of CF_3CO_2 that are due to the ν_{CO_2} stretch modes are quite weak. This suggests that the CF_3CO_2 is adsorbed roughly parallel to the surface such that neither of these two modes has significant projections onto the surface normal. The HREEL spectra support the proposal that $\text{CF}_3\text{CO}_2\text{H}$ deprotonates during heating on the clean $\text{Ag}(110)$ surface to produce CF_3CO_2 .

The vibrational spectra of the $\text{CF}_3\text{CO}_2\text{H}$ monolayer on the $\text{Ag}(111)$ surface and the species remaining after heating the monolayer to 300 K have been obtained using FT-IRRAS and are shown in Figure 11. These are much simpler than the HREEL spectra on the $\text{Ag}(110)$ surface, and the assignments have also been made by comparison

(26) Fuson, N.; Josien, M.-L.; Jones, E. A.; Lawson, J. R. *J. Chem. Phys.* **1952**, *20*, 1627.

(27) Robinson, R. E.; Taylor, R. C. *Spectrochim. Acta* **1962**, *18*, 1093.

(28) Spinner, E. *J. Chem. Soc.* **1964**, 4217.

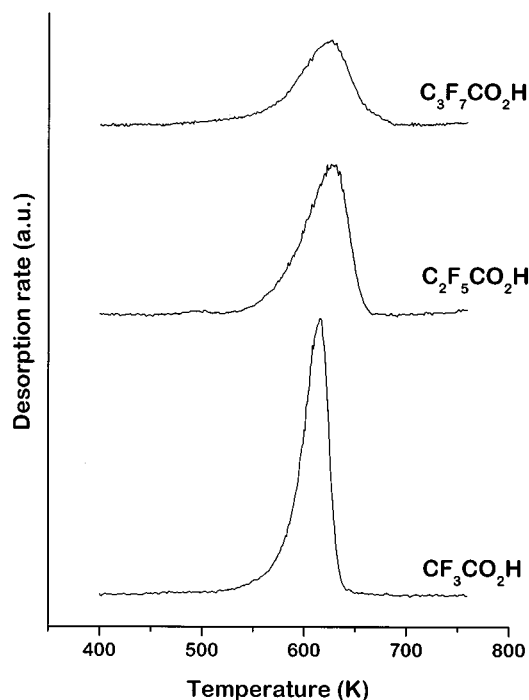
TPRS - $F(CF_2)_nCO_2H / Ag(110)$ 

Figure 7. TPRS spectra of $F(CF_2)_nCO_2H$ ($n = 1-3$) on the Ag(110) surface. These reveal the higher temperature desorption feature (620 K) due to decomposition of perfluorocarboxylate groups on the surface. The heating rate was 5 K/s, and the fragment monitored was at $m/q = 44$.

Table 1. Vibrational Frequencies (cm^{-1}) and Assignments for Modes Observed in the HREELS and FT-IRRAS Spectra of CF_3CO_2H Adsorbed on the Clean Ag(110) and Ag(111) Surfaces, Respectively, at 90 K

mode	$CF_3CO_2H(g)^{25}$	$CF_3CO_2H/Ag(110)$ multilayer	$CF_3CO_2H/Ag(111)$ monolayer
ρ_{CF_3}	267, 467	300, 400	
δ_{OCO}	708	710	
ν_{CC}	825	890	
γ_{OH}	1123		
$\nu^s_{CF_3}$	1182	1210	1205
ν_{C-O}, δ_{OH}	1203		
$\nu^a_{CF_3}$	1244		1247
δ_{C-O}	1465	1500	
$\nu_{C=O}$	1788	1780	1781
$\delta_{OCO} + \nu_{CF_3}$		1920	
$\nu_{CC} + \nu_{CF_3}$		2100	
$2\nu_{CF_3}$		2450	
ν_{OH}	2700-3248	3020	

with the vibrational spectra of gas-phase CF_3CO_2H and aqueous $CF_3CO_2^+$. The spectrum of the CF_3CO_2H monolayer reveals features due to both the $\nu_{CF_3}^s$ and $\nu_{CF_3}^a$ modes that are resolvable with FT-IRRAS. In addition, the absorption due to the $\nu_{C=O}$ mode is visible at 1781 cm^{-1} . After heating to 300 K there is only a single absorption that is assigned to the $\nu_{CF_3}^a$ mode. The fact that it is red-shifted by 30 cm^{-1} from the spectrum of the CF_3CO_2H monolayer at 90 K is consistent with the conversion of the adsorbed species into CF_3CO_2 . In addition, the fact that only absorption due to the $\nu_{CF_3}^a$ mode is observed and there are no absorptions due to the $\nu_{CF_3}^s$ or the ν_{CO_2} modes is consistent with the formation of a species lying with its plane roughly parallel to the Ag(111) surface. In summary, all the spectroscopic evidence points toward a reaction of

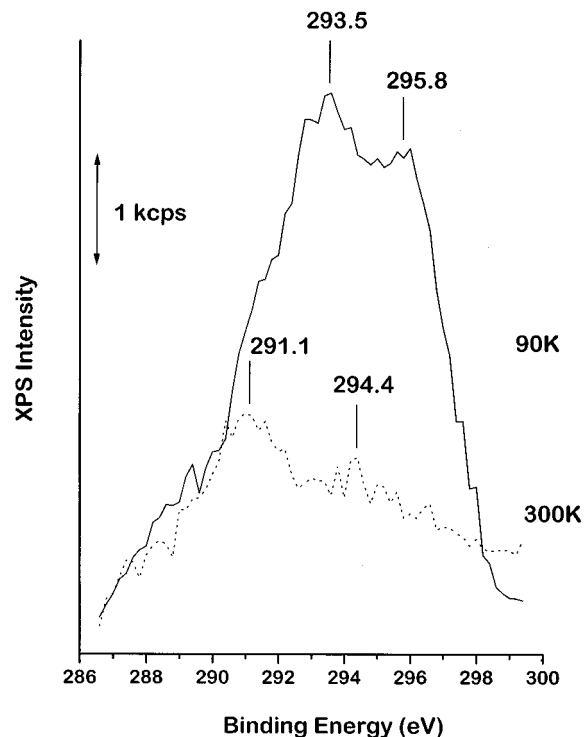
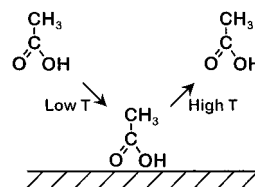
XPS - C 1s $CF_3CO_2H / Ag(111)$ 

Figure 8. XPS of the C 1s region for a monolayer of CF_3CO_2H adsorbed on the Ag(111) surface at 90 K and for the surface after heating to 300 K. The spectrum at 90 K reveals poorly resolved features due to the $-CO_2H$ group (binding energy of 293.5 eV) and due to the $-CF_3$ group (binding energy of 295.8 eV). Heating to 300 K causes the desorption of roughly 75% of the adsorbed monolayer of CF_3CO_2H and leaves CF_3CO_2 with binding energies of 291.1 eV ($-CO_2$) and 294.4 eV ($-CF_3$). The shoulder on the low binding energy side of the spectrum obtained at 90 K suggests that there may already be some CF_3CO_2 on the surface at 90 K.

CF_3CO_2H to form CF_3CO_2 on both the clean Ag(110) and Ag(111) surfaces.

4. Discussion

4.1. Surface Reaction Mechanism of Acids on Ag(110) and Ag(111). The results presented in the previous section provide a clear picture of the reaction mechanism of the hydrocarbon carboxylic acids on the Ag(110) and Ag(111) surfaces that is consistent with previous observations made using formic acid (HCO_2H) and CH_3CO_2H on the Ag(110) surface.^{9,11} CH_3CO_2H adsorbs and desorbs reversibly on both the Ag(110) and Ag(111) surfaces as illustrated below.



Furthermore, on the Ag(110) surface we observe that all the straight-chain hydrocarbon acids from acetic through to hexanoic acid desorb from the surface during heating without any evidence of deprotonation or decomposition. The only differences among the straight-chain acids are

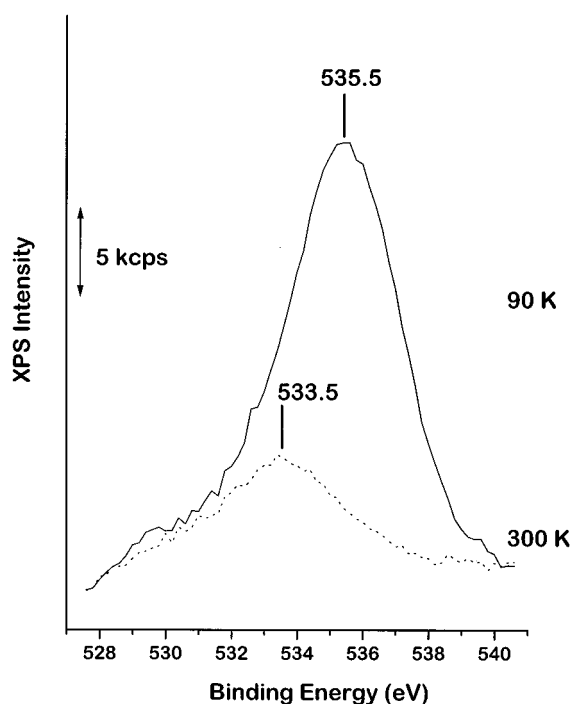
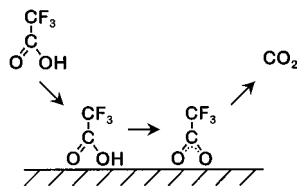
XPS - O 1s CF₃CO₂H / Ag(111)

Figure 9. XPS of the O 1s region for a monolayer of CF₃CO₂H adsorbed on the Ag(111) surface at 90 K and for the surface after heating to 300 K. The spectrum obtained at 90 K reveals one peak due to the -CO₂H group with a binding energy of 535.5 eV. After heating to 300 K roughly 75% of the adsorbed monolayer desorbs, leaving CF₃CO₂ on the surface with an O 1s binding energy of 533.5 eV.

that the monolayer desorption energies²⁹ increase with increasing alkyl chain length. The dependence on the alkyl chain length, n , is given by the expression $\Delta E_{\text{des}} = 10.6 + 0.9n$ kcal/mol. The value of the desorption energy increment is similar to that for the interaction of straight chain alcohols with the Ag(110) surface for which the desorption energy increment is 1.1 kcal/mol/CH₂³⁰ and that for alkyl groups on Cu(111) surfaces for which the desorption energy is incremented by 1.3 kcal/mol/CH₂.³¹ Ultimately, the point of this work has been to probe the nature of the transition state for the deprotonation of the acids. The desorption energy for hexanoic acid is 15.1 kcal/mol and represents a lower limit on the barrier to deprotonation, $\Delta E_{\text{dep}}^{\ddagger}$, of the hydrocarbon carboxylic acids.

The fluorinated acids all appear to deprotonate on the Ag(110) and Ag(111) surface during heating. In the case of CF₃CO₂H the spectroscopic evidence suggests that, as expected, the deprotonation product is adsorbed CF₃CO₂.



On the Ag(111) surface there is some desorption of the CF₃CO₂H monolayer at ~225 K. The deprotonation of CF₃-CO₂H must occur at lower temperatures to yield CF₃CO₂.

(29) Redhead, P. A. *Vacuum* **1962**, *12*, 203.

(30) Zhang, R.; Gellman, A. J. *J. Phys. Chem.* **1991**, *95*, 7433.

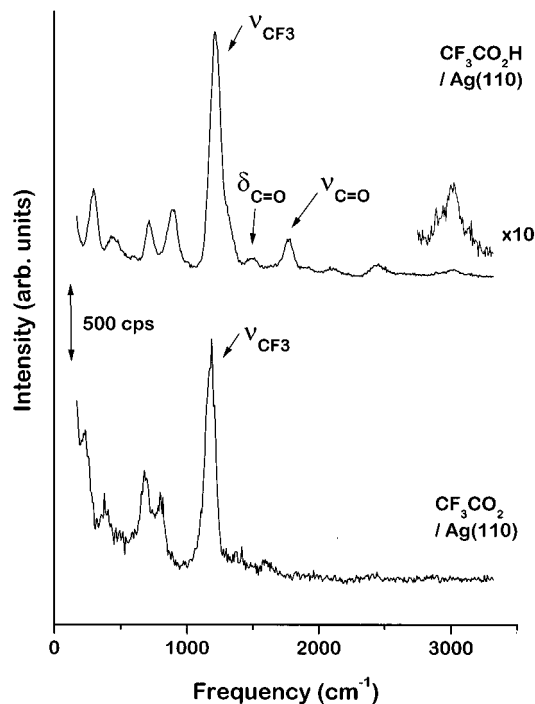
HREELS - CF₃CO₂H & CF₃CO₂ / Ag(110)

Figure 10. HREEL spectra of a CF₃CO₂H multilayer on Ag(110) at 90 K and of CF₃CO₂ on Ag(110) after heating to 500 K. The disappearance of the feature at 3020 cm⁻¹ indicates deprotonation of the CF₃CO₂H to CF₃CO₂. Both spectra were obtained at 90 K. The spectral resolution for the elastic peaks were 80 cm⁻¹ for CF₃CO₂H and 68 cm⁻¹ for CF₃CO₂.

Table 2. Vibrational Frequencies (cm⁻¹) and Assignments for Modes Observed in the HREELS and FT-IRRAS Spectra of CF₃CO₂ on the Clean Ag(110) and Ag(111) Surfaces

mode	CF ₃ CO ₂ ⁻ aq soln ^{26,27}	CF ₃ CO ₂ /Ag(110)	CF ₃ CO ₂ /Ag(111)
$\nu_{\text{Ag-O}}$		230	
ρ_{CF_3}	267, 437	390	
δ_{OCO}	726	690	
ν_{CC}	844	800	
$\nu^{\text{s}}_{\text{CF}_3}$	1143		
$\nu^{\text{a}}_{\text{CF}_3}$	1202	1180	1210
$\nu^{\text{s}}_{\text{CO}_2}$	1435		
$\delta^{\text{a}}_{\text{CO}_2}$	1681		

which is stable on the surface to temperatures of ~620 K at which point it decomposes to generate CO₂ and other desorption fragments. On the Ag(110) surface the longer chain, perfluorinated carboxylic acids CF₃CF₂CO₂H and CF₃CF₂CF₂CO₂H both appear to undergo deprotonation during heating to form the corresponding perfluorinated carboxylates. The implication of these results is that fluorination of the alkyl chain must lower $\Delta E_{\text{dep}}^{\ddagger}$ to the point that it is lower than ΔE_{des} .

4.2. Transition State for Acid Deprotonation on Ag(111) and Ag(110). The basic observation of this work is that while the hydrocarbon carboxylic acids are adsorbed reversibly, the perfluorinated carboxylic acids deprotonate during heating on the clean Ag(111) and Ag(110) surfaces. This observation can be used to make some inferences concerning the nature of the transition state for the deprotonation reaction on these surfaces. The fact that the hydrocarbon acids desorb rather than deprotonating implies that $\Delta E_{\text{dep}}^{\ddagger}$ is higher than ΔE_{des} . The longest chain hydrocarbon acid to be studied was hexanoic acid, which

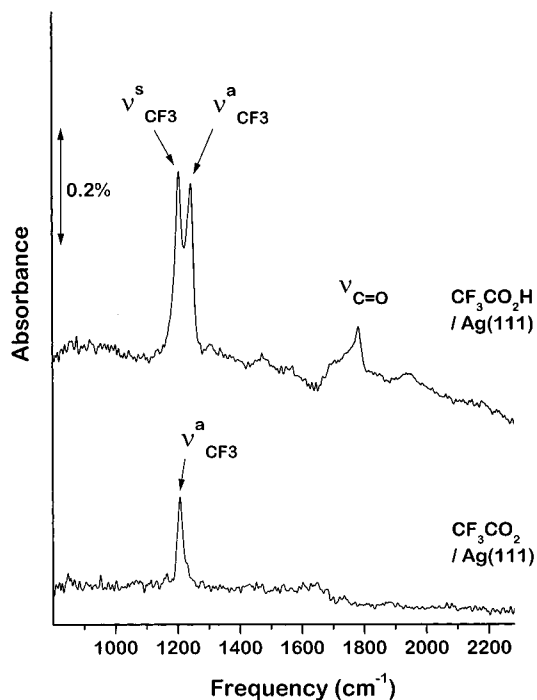
FT-IRRAS - CF₃CO₂H & CF₃CO₂ / Ag(111)

Figure 11. FT-IRRAS of the CF₃CO₂H monolayer on Ag(111) at 90 K and of CF₃CO₂ on Ag(111) after heating to 300 K. The spectrum of the CF₃CO₂ on the surface reveals an absorption due to the ν^aCF₃ mode alone. The fact that no absorption is observed due to the ν^sCF₃ mode or either of the -CO₂ modes suggests that the CF₃CO₂ is adsorbed with its molecular plane roughly parallel to the surface.

has a desorption energy of $\Delta E_{\text{des}} = 15.1$ kcal/mol. This implies that the barrier to deprotonation is $\Delta E_{\text{dep}}^{\ddagger} > 15.1$ kcal/mol. Assuming that $\Delta E_{\text{dep}}^{\ddagger}$ is not greatly affected by the alkyl chain length of the acids, then for all the acids, including CH₃CO₂H, $\Delta E_{\text{dep}}^{\ddagger} > 15.1$ kcal/mol. The assumption that $\Delta E_{\text{dep}}^{\ddagger}$ is not greatly affected by increasing the length of the alkyl group is reasonable since it is known that the gas phase heat of deprotonation decreases by ~0.7 kcal/mol as methylene groups are added to CH₃-CO₂H.⁸ The fact that it decreases strengthens our argument that for CH₃CO₂H, $\Delta E_{\text{dep}}^{\ddagger} > 15.1$ kcal/mol. The energetics for acid deprotonation on the Ag surfaces are illustrated in the potential energy diagram of Figure 12. This figure shows the energies for desorption and for deprotonation of the hydrocarbon and fluorocarbon acids. Note that the discussions in this work are all in terms of energy differences ($\Delta E_{\text{dep}}^{\ddagger}$ or ΔE_{des}). We have chosen the adsorbed state for the acids on the surfaces as the reference energy state against which to plot all energy differences.

The fact that the perfluorinated carboxylic acids deprotonate rather than desorb from the clean Ag(111) and Ag(110) surfaces implies that the $\Delta E_{\text{dep}}^{\ddagger} < \Delta E_{\text{des}}$. The fact that on the Ag(111) surface we have observed both the desorption and the deprotonation of CF₃CO₂H suggests that the barriers to these two processes are roughly equivalent and that the two processes compete with one another. The desorption temperature of CF₃CO₂H is 225 K and yields a desorption energy of $\Delta E_{\text{des}} = 13.5$ kcal/mol. The net implication is that for the deprotonation of CF₃-CO₂H on the Ag surfaces $\Delta E_{\text{dep}}^{\ddagger} \leq 13.5$ kcal/mol. The lower bound on the $\Delta E_{\text{dep}}^{\ddagger}$ for CH₃CO₂H and the upper bound

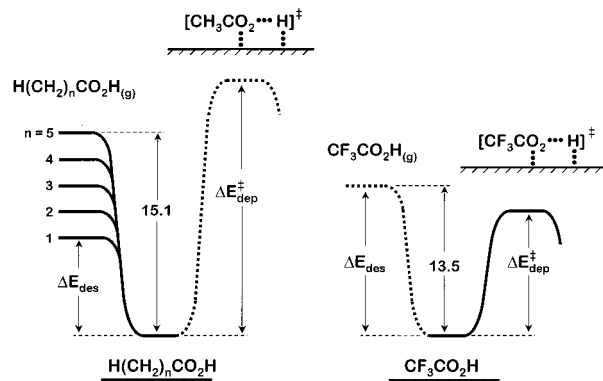


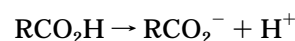
Figure 12. Potential energy diagram showing the adsorption and/or deprotonation of the hydrocarbon acids (left) and the fluorocarbon acids (right) on the Ag(111) or Ag(110) surfaces. The potential energy surfaces followed by the adsorbates are shown as solid lines while the potential energy surface for the higher energy pathways are shown as dashed lines. The fact that the hydrocarbon acids all desorb from the surface indicates that $\Delta E_{\text{dep}}^{\ddagger} > 15.1$ kcal/mol, which is the ΔE_{des} of hexanoic acid. The fact that the fluorinated acids deprotonate indicates that $\Delta E_{\text{dep}}^{\ddagger} \leq 13.5$ kcal/mol, which is the desorption energy for CF₃-CO₂H. The net result is that $\Delta E_{\text{dep}}^{\ddagger}(\text{CF}_3\text{CO}_2\text{H}) < \Delta E_{\text{dep}}^{\ddagger}(\text{CH}_3\text{CO}_2\text{H})$.

on the $\Delta E_{\text{dep}}^{\ddagger}$ of CF₃CO₂H show that

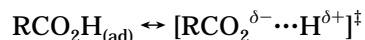
$$\Delta E_{\text{dep}}^{\ddagger}(\text{CF}_3\text{CO}_2\text{H}) < \Delta E_{\text{dep}}^{\ddagger}(\text{CH}_3\text{CO}_2\text{H})$$

The desorption energies and deprotonation barrier for CF₃-CO₂H on the Ag(111) and Ag(110) surface are illustrated in Figure 12. The effect of fluorination on the methyl group is to lower the $\Delta E_{\text{dep}}^{\ddagger}$ by at least 1.6 kcal/mol.

The lowering of the $\Delta E_{\text{dep}}^{\ddagger}$ of RCO₂H on the Ag surfaces by fluorination of the alkyl group is consistent with the effects of fluorination on gas phase and solution phase acidities. Fluorination of the methyl group lowers the gas phase heat of deprotonation of CH₃CO₂H by 25 kcal/mol while in aqueous solution it is lowered by 1.7 kcal/mol.^{8,32} This is due to the fact that fluorination of the methyl group stabilizes the carboxylate anion product of the deprotonation reaction.

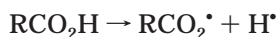


For the acetic acids this effect is a reflection of the fact that the field substituent constant of the CF₃ group, $\sigma_{\text{F}}^-(\text{CF}_3) = 0.44$, is much greater than that of the CH₃ group, $\sigma_{\text{F}}^-(\text{CH}_3) = 0.0$.^{33,34} It is tempting to use this comparison of the effects of fluorine on the gas phase and surface deprotonation energetics to suggest that the deprotonation reaction on the Ag surfaces has a transition state that is anionic with respect to the adsorbed acid.



However, it is important to point out that the fluorination also influences the energetics for gas-phase homolytic cleavage of the O-H bond.

- (31) Lin, J. L.; Bent, B. E. *J. Phys. Chem.* **1992**, *96*, 8529.
 (32) Isaacs, N. S. *Physical Organic Chemistry*, 2nd ed.; Longman Scientific & Technical: Essex, UK, 1995; p 239. Henne, A. L.; Fox, C. J. *J. Am. Chem. Soc.* **1951**, *73*, 2323.
 (33) Hansch, C. A.; Leo, A.; Taft, R. W. *Chem. Rev.* **1991**, *91*, 165.
 (34) Taft, R. W.; Topsom, R. D. *Prog. Phys. Org. Chem.* **1987**, *16*, 1.



Fluorination of the methyl group lowers the homolytic bond dissociation energy from 105 to 103 kcal/mol. This decrease by 2 kcal/mol falls within the bounds of the effects of fluorination that we have measured on the Ag surfaces. Thus, these measurements do not yet enable us to distinguish between heterolytic and homolytic descriptions of the transition state to acid deprotonation on the Ag surfaces.

Although we know at this point that fluorine substitution of the alkyl groups in carboxylic acids lowers $\Delta E_{\text{dep}}^\ddagger$ on the clean Ag surfaces, the magnitude of the effect is still unknown. The value of $\Delta E_{\text{dep}}^\ddagger$ for $\text{CF}_3\text{CO}_2\text{H}$ on the Ag(111) surface is probably of the same order as the $\Delta E_{\text{des}} = 13.5$ kcal/mol. However, for $\text{CH}_3\text{CO}_2\text{H}$ and the other hydrocarbon carboxylic acids we can estimate only a lower limit on $\Delta E_{\text{dep}}^\ddagger$ of 15.1 kcal/mol. In the future, direct measurements of carboxylic acid deprotonation kinetics would be very interesting in order to put a firm value on the difference in $\Delta E_{\text{dep}}^\ddagger$ between the hydrocarbon and fluorocarbon acids. This is probably best accomplished by studying the kinetics of the deprotonation process on a

surface on which both $\text{CH}_3\text{CO}_2\text{H}$ and $\text{CF}_3\text{CO}_2\text{H}$ are known to deprotonate. At that point it would be possible to compare the fluorine substitution effects with those observed in other environments such as the gas phase or solution phase.

5. Conclusion

The $\Delta E_{\text{dep}}^\ddagger$ is lower for $\text{CF}_3\text{CO}_2\text{H}$ than that for $\text{CH}_3\text{CO}_2\text{H}$ on the Ag(110) and Ag(111) surfaces. As a result, $\text{CF}_3\text{CO}_2\text{H}$ deprotonates on the clean Ag surfaces under conditions in which the $\text{CH}_3\text{CO}_2\text{H}$ simply desorbs into the gas phase. The product of the deprotonation of $\text{CF}_3\text{CO}_2\text{H}$ on the Ag(111) and Ag(110) surfaces has been identified as a CF_3CO_2 group that appears to be adsorbed with its molecular plane roughly parallel to the surface. The fact that fluorination of the methyl group lowers the $\Delta E_{\text{dep}}^\ddagger$ is consistent with its effects on both gas-phase deprotonation and homolytic cleavage of the O–H bonds of acetic acids.

Acknowledgment. This work has been supported by NSF Grant CHE-0091765.

LA011103D